J. Innovative Eng. Nat. Sci., vol. 5, no. 1, pp. 1-18, 2025.
http://doi.org/10.61112/jiens.1514611

Journal of Innovative Engineering and Natural Science
(Yenilikçi Mühendislik ve Doğa Bilimleri Dergisi)
https://dergipark.org.tr/en/pub/jiens

Original Paper

The effect of positioning of seismic isolators in a reinforced concrete building

Muhammet Yurdakul[a,*] and Mehmet Burak Yıldız[b]

[a]Karadeniz Technical University, Faculty of Technology, Department of Civil Engineering, Trabzon and 61830, Türkiye.
[b]BETAŞ Prefabricated, Isparta and 32000, Türkiye.

ARTICLE INFO

Article history:
Received
Received in revised form
Accepted

Available online

Keywords:
HDRB design
UBC97
Isolator device positioning
Reinforced concrete building
Finite elements model

ABSTRACT

Construction costs are increasing day by day. The importance of building the safest structures at the lowest cost is also increasing. For this purpose, it is necessary to design the structure in the best possible way without sacrificing safety. One way to ensure buildings are safe even during severe earthquakes is to include seismic isolation at the design stage. Judging by studies, seismic isolators are generally located at the lowest story of the building. However, there is no sufficient study to determine the location of the seismic isolator in the lowest column. In this study, the seismic isolator was located at the lower end and the top of the lowest story of the RC building to compare the effectiveness of its positioning. A high-damping rubber bearing (HDRB) was used as the seismic isolation device. Also, the effect of the absence of the diaphragm placed above the isolation level was investigated. As a result of the study, the necessary rebar of the RC building isolated at the top end of the column was less than 15% compared to the building isolated at the lower end of the columns for the beams. The base shear force of the building with seismic isolator located at the upper end of the column was 2.7% greater than that the building with the seismic isolator located at the lower end of the column.

I. INTRODUCTION

Humankind, learning lessons from earthquakes for centuries, has developed various methods to make structures safer. They have developed the idea of separating the ground and the structure. There are several applications in this regard. As an example, a seismic isolation system based on separating the building and ground is applied to the building through various methods. In this application, the aim is to extend the building period, reduce the earthquake load, and decrease the relative floor displacement. Seismic isolation leads to slight damage in the case of strong ground motion excitations.

Ryan and Earl [1] examined the effectiveness of seismic isolation systems placed between floors as a function of their location and studied alternative approaches to select their properties. The study showed that single-story isolation systems reduced the forces on the isolation system. However, it was not effective in reducing the forces under the isolation system. Huang et al. [2] carried out experimental research on mid-story seismic isolated structures. Laminated rubber bearings were used as the isolation system. The responses of the mid-story and fixed structures were compared. Shadzad et al. [3] propose a new configuration for the Mega-Subcontrolled Structural System used in high-rise buildings, incorporating an inverted V-bracing and a mid-story isolation system. Based on the analysis of structural responses to seven different seismic waves, this new configuration shows a 49.7% improvement in structural acceleration response. Shu et al. [4] evaluate the seismic performance of a new staggered story isolated structure using numerical simulations and damage index calculations, analyzing the effects of different upper isolated layer positions and chassis areas. Results show that lowering the upper isolated layer

*Corresponding author. Tel.: +90-536-640-3184; e-mail: m.yurdakul@ktu.edu.tr

reduces inter-layer shear force, acceleration, and displacement, improving energy dissipation and reducing core tube damage. While increasing the chassis area improves isolation effects above the upper layer, it increases shear force and acceleration below it, but the structure's displacement, tensile, and compressive stresses remain within standard limits under seismic conditions. Di Egidio et al. [5] focused on the seismic performance of frame structures incorporating inter-storey isolation, a technique where stiffness-altering devices are placed at higher storey levels rather than the base. An elasto-plastic discontinuity, modelled using the Bouc-Wen approach, is introduced in the structure and analyzed through a 3-DOF reduced model under harmonic and seismic excitations. Results are presented as gain maps to identify parameters that optimize the seismic behaviour of the structure. Skandalos et al. [6] presented a multi-objective optimization analysis of inter-story isolation. Authors placed the seismic isolation devices between stories to control the building's response while reducing the load on the isolation layers. Random vibration analysis was employed to minimize the maximum inter-story drift ratio and isolation drift, optimizing the placement and properties of the isolation layers.

Charmpis et al. [7] and Zhou et al. [8] studied the optimization of earthquake response with seismic isolation at different story levels. The optimization aimed to minimize the response of the building. Wang et al. [9] investigated the dynamic characteristics and seismic responses of mid-story isolated buildings. They found out that the stiffness and mass of the superstructure were significantly lower than those of the substructure, affecting the dynamic characteristics of the isolated building. Wang et al. [10] experimentally investigated the dynamic behaviour of a building with base and mid-story isolation systems. The analysis results showed that a mid-story isolated building had smaller fundamental modal quantities than a base-isolated building. Kim and Kang [11] pointed out that both the peak story and isolator drifts conflict with each other in a mid-story isolation building. To solve this problem, they suggested a smart mid-story isolation system. Faiella and Mele [12] investigated two different mid-story isolated buildings to interpret the latest design practice. Non-linear time history and modal analyses were carried out on simplified models for seismic assessment.

The inter-story isolation system, or in other words, the mid-story isolation system, was used in real buildings in Japan, but there were some design problems [12]. Although the above studies and studies including the mid-story isolation system [13-17] were experimental, numerical base isolation systems are used in real buildings. By considering this, this study was performed about the base isolation system.

The studies in which the seismic isolation system was placed on mid-story were mentioned above. A base isolation system is generally located on the lowest column of the building. Also, in most seismic base isolation applications, a relatively rigid diaphragm is constructed above the isolators. There is insufficient research on the effectiveness of seismic isolation systems at different levels of the building's lowest columns, and on the use of rigid diaphragms at isolation levels. To eliminate this insufficient in the literature, this study's aim to determine the effects which column level the isolation system is more effective, and the absence of the diaphragm placed above the isolation level. For this purpose, the seismic isolators were located at the lower end of the columns (LEC) and the top end of the columns (TEC), and rigid diaphragm was not used in the dynamic analyses. In the study, the periods of a reinforced concrete building, story displacements, column shear forces, base shear forces, and the required reinforcement amounts for beams were compared. Additionally, evaluations were made from an architectural usability perspective. A 3D finite element model of a seven-story reinforced concrete (RC) isolated building was modelled in SAP2000. Response spectrum analyses were performed for assessment of the dynamic behaviour of

the RC building. The isolation system was designed according to UBC-97 [19]. This code is still frequently referred to in the design of seismically isolated buildings around the world [20].

II. MATERIAL AND METHOD

2.1 Seismic Isolator Design Principles

In UBC-97, regions are divided into five according to their seismic activity. While the 1st earthquake zone represents the lowest, the 4th earthquake zone represents the highest seismic activity. The acceleration value obtained from the map created by EMPED for the region where the building will be built is 0.308 g. Therefore, the seismic zone factor, Z, was selected as 4 according to UBC-97 Table 16-I. Since the area where the building is located has firm soil, the soil profile type was selected as SD according to UBC-97 Table 16-J. In UBC-97, the seismic source type is classified as A, B, or C according to the seismic risk carried by the fault. Since the building is close to the 1st earthquake zone and faults that may cause large earthquakes, the seismic source type was selected as "A" according to Table 16-U in UBC-97. Since the closest distance of the building to the seismic source was more than 15 km, the near-source factors Nv and Na were selected as 1 according to Table 16-S and 16-T in UBC-97, respectively. There are two types of seismic coefficients, which are Ca and Cv. Seismic zone factor, soil profile type, and near-source factor were previously selected as 0.4, SD, and 1, respectively. With these selected values, the seismic coefficient Ca was selected as 0.44 Na according to Table 16-Q in UBC-97.

Similarly, the seismic coefficient CVD was selected as 0.64NV according to Table 16-R in UBC-97. When Nv is equal to 1, CVD was found to be 0.64. Maximum capable earthquake response coefficient (MCERC), MM, was found to be 1.25 according to Table A-16-D in UBC-97 depending on the design basis earthquake shaking intensity. ZNV was equal to 0.4 (0.4*1=0.4). CAM and CVM seismic coefficients used to define the minimum spectral ordinates of the MCERC spectrum with constant acceleration and rapid parts were obtained from Table A-16-F and Table A-16-G in UBC-97 based on the vibration intensity and the soil profile type as 0.55 and 0.80, respectively. The damping coefficient of the isolation system with a damping ratio of 10% was obtained as 1.2 from Table A-16-C in UBC-97. Since the structural system of the isolated building will have moment-resisting frames, the earthquake reduction coefficient, R1, was selected as 2 from UBC-97 Table 16-N and Table A-16-R.

In case of research driven by experimental study, test procedure / method should be explained in a clear way. If a theoretical study has been carried out, the theoretical method should be given in detail. If the method has been previously mentioned in published studies, the difference of the current study should be stated by referring to the previous studies.

2.2 Selected Building Design

UBC-97 was used to design the isolation system. The building was designed according to TBEC2018 [21]. Since the location of the building was assumed to be in Turkey, the spectrum curve for that location was used. The spectrum curve as seen Table 1 for that location was obtained according to TBEC 2018 [21]. There are studies about the time history of the seismic evaluation or in pushover analysis where the isolator was designed according to UBC97 [22-23]. There are four stories on the 1–7 axes of the building and seven stories on the 7–11 axes. The

axis distances in both directions of the building were 7 m (Fig. 1). A 3D finite element model of the building is given in Fig. 2.

The model consists of 13672 nodal points, 987 frames, and 71 link elements. An RC frame system was used as the structural system. The RC-framed building was modelled with a slab plate. The floor was defined as a rigid diaphragm. C30 and S420 were used as a concrete class and steel rebar class, respectively. Column, beam dimensions, and floor slab thickness were 80x80 cm, 40x70 cm, and 15 cm, respectively.

The peak ground acceleration of the region where the analysed building will be located is 0.308 g, the short- period map spectral acceleration coefficient (SS) is 0.728. The map spectral acceleration coefficient (S1) for the 1 second period was selected from the earthquake hazard map as 0.168 according to the new earthquake hazard map of Turkey [21].

The story height of the building was chosen as 4 m. Two different analyses were carried out in the seismically isolated building by locating high-damping rubber bearing (HDRB) at the LEC and TEC at the foundation level (Fig. 3). In the design of the HDRB, the vertical load transmitted to the ground was taken into consideration, and the difference in weight between the bottom of the column and the top of the column was neglected. The live and dead loads were 5 kN/m^2 and 1 kN/m^2, respectively [24]. In earthquake calculations, the active load participation ratio was considered to be 30%.

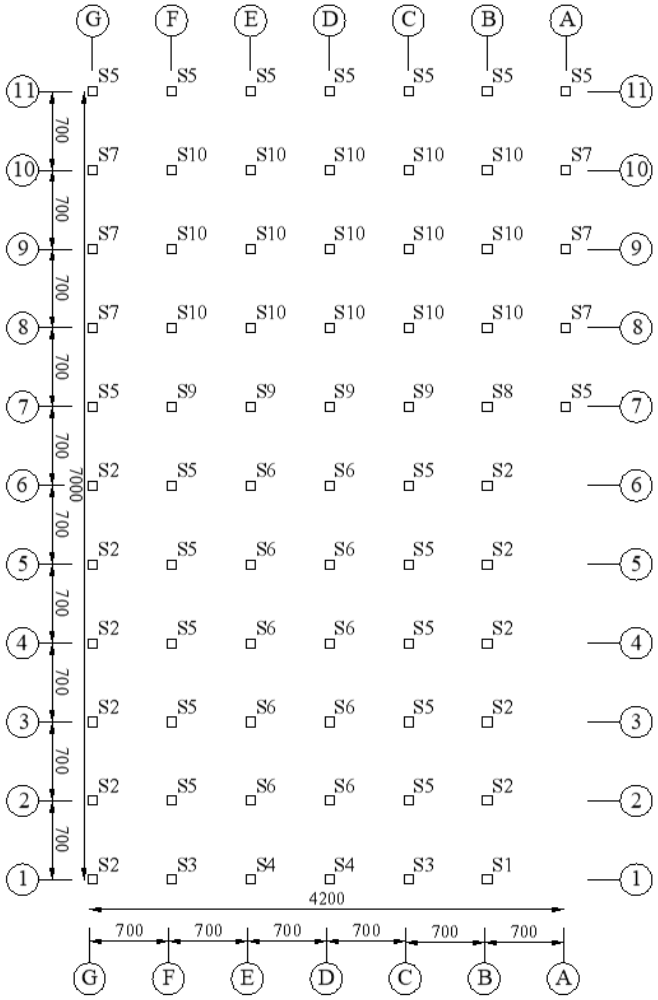

Figure 1. Plan of the location of seismic isolators (S_i represents the name of the isolator, i=1,2,3,…..10)

Table 1. Parameters and graphs of design acceleration spectrum

Parameters	Value	Function Graphs
0.2 sec spectral acceleration, S_s	0.728	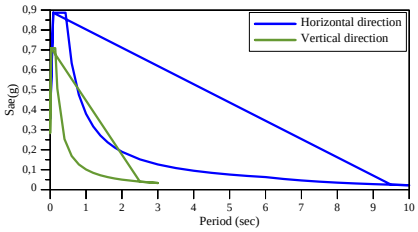
1 sec spectral acceleration, S_1	0.168	
Long-period transition period	6.0	
Response modification, R	2.0	
Site class	ZD	
Site coefficient, F_s	1.2176	
Site coefficient, F_1	2.264	
Design spectral acceleration, S_{DS}	0.8864	
Design spectral acceleration, S_{D1}	0.3804	

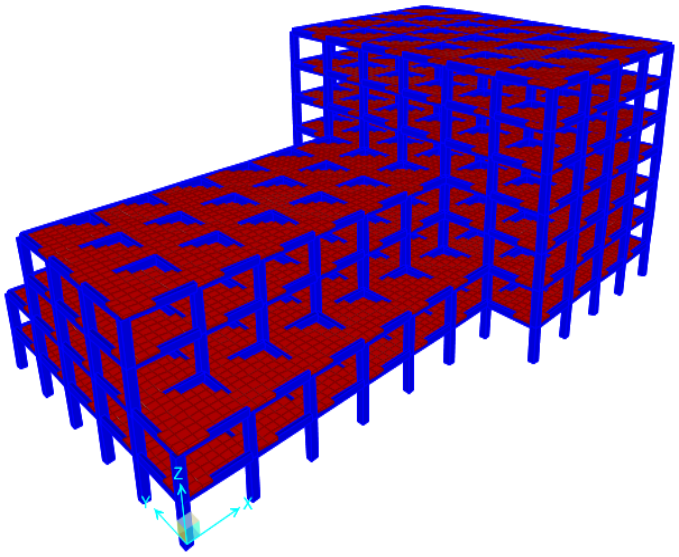

Figure 2. 3D finite element model of the building

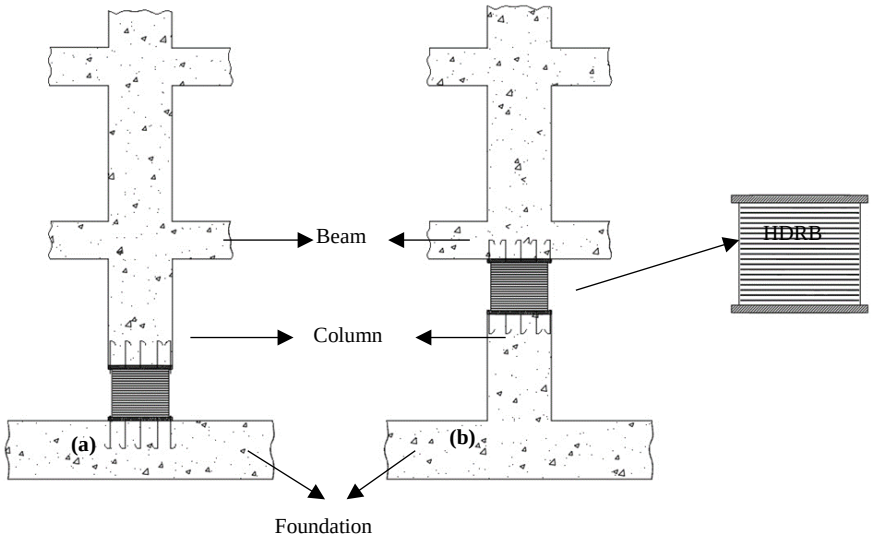

Figure 3. Detail of the placement of HDRB at LEC (a) and TEC (b)

The building importance coefficient was taken as 1 by the regulation of the isolated building. When calculating the building weight, the unit volume weight of reinforced concrete and wall weight were 25 kN/m^3 and 4 kN/m, respectively.

2.3 Design of HDRB system

In this study, HDRB was chosen because it provides the necessary flexibility and damping without any additional elements. In addition, it has a straightforward design and easy production. The first vibration period of the fixed building was determined to be 0.93 s. The targeted period (TD) was 2.8 s which was three times more than the fixed period of the building, and the maximum period of the building was 3.5 s. Seventy-one isolators were used, and shear modulus (G) of the isolators was set to 1 MPa. Nine different isolators were designed to seismically analyze the isolated building. The total weight of the building (g+0.3q) was 156600 kN. Axial forces supported by columns are given in Table 2.

The torsional effects of the building were reduced by placing high rigidity HDRB between the 7-11 axis. The isolator devices were placed so that the center of mass and the center of rigidity were as close as possible. The torsional irregularity control was made according to TBEC 2018 [21] for the seismically isolated building. For a single selected type of isolator, the following design steps used the equations in UBC97. Design displacement, DD, was calculated by Eq. 1.

Table 2. Axial forces supported by columns

Column Type	Axial force (kN)	Number of Column
S1	500	2
S2	700	10
S3	1100	2
S4	1400	2
S5	1800	14
S6	2150	10
S7	2400	11
S8	2600	1
S9	3100	4
S10	3700	15

$$D_D = \frac{g \times C_{VD} \times T_D}{B \times 4\pi^2} \quad (1)$$

Maximum displacement, D_M, was calculated by Eq. (2).

$$D_M = \frac{g \times C_{VM} \times T_M}{B \times 4\pi^2} \quad (2)$$

C_{VD} and C_{VM} are seismic coefficients, B is the damping coefficient, and g is the gravitational acceleration. Design and maximum displacements were calculated as 0.371 m and 0.579 m according to Eqs. (1-2), respectively. Minimum horizontal stiffness, k_D, was calculated by Eq. (3).

$$k_D = \frac{4\pi^2 \times W}{{T_D}^2 \times g} \quad (3)$$

where W is the axial force supported by the bearing.

The HDRB used as an isolation system can change shape up to 150% of its thickness. Accordingly, the total rubber thickness of the isolator was calculated by Eq. (4).

$$t_r = \frac{D_D}{\Upsilon} \tag{4}$$

where tr is thickness and ϒ is the strain coefficient of the isolator. The thickness of the isolator was calculated as 0.3 m. The minimum isolator diameter was calculated by Eq. (5).

$$A = \frac{k_D \times t_r}{G} \tag{5}$$

Horizontal stiffness and total horizontal stiffness were calculated by Eqs. (6) and (7), respectively.

$$K_H = \frac{A_1 \times G}{t_r} \tag{6}$$

$$\Sigma K_H = N_A \times K_H^A + N_B \times K_H^B + \cdots \tag{7}$$

Where KH is the horizontal stiffness and N is the number of the isolator. Total horizontal stiffness was calculated to be 87560 kN/m. The effective vibration period of the system was calculated by Eq. (8).

$$T_E = 2\pi \sqrt{\frac{W_T}{\sum K_H \times g}} \tag{8}$$

where T_E is the effective vibration period and calculated as 2.68 s. Since this value was close to the target period, calculations continued. The total damping and the damping coefficient were calculated by Eq. (9) and Eq. (10), respectively.

$$B = \frac{\sum(N \times {K_H}^1 \times B + N \times {K_H}^2 \times B + \cdots + N \times {K_H}^9)}{\sum K_H} \tag{9}$$

$$\beta = \frac{4}{1 - \ln B} \tag{10}$$

where B is total damping and β is the damping coefficient. Total damping was calculated as 10%, and the damping coefficient was calculated as 1.21. Real horizontal displacement of the building according to changing damping ratios was calculated by Eq. (11).

$$D_D = \frac{g \times C_v \times T_E}{B \times 4\pi^2} \tag{11}$$

Real horizontal displacement was calculated as 0.37 m. Since the thickness of the isolator was 30 cm, horizontal displacement was within the desired limits. The maximum displacement of the isolator occurred due to torsion. Eqs. (12-14) were used to calculate it.

$$E = 0{,}05 \times e \tag{12}$$

$$D_{total} = D_D \left(1 - \frac{12 \times E}{b^2 + d^2} \right) \tag{13}$$

$$D_{total} \geq D_D \times 1{,}1 \tag{14}$$

where e is the long side of the building plan, and b and d are the dimensions of the building in the X and Y direction. Maximum displacement was calculated as 0.39 m. The base shear force of the isolated building was calculated with Eqs. (15-17).

$$V_b = K_H \times D_D \tag{15}$$

$$V_S = \frac{K_H \times D_D}{R} \tag{16}$$

$$C_S = \frac{V_s}{W_T} \tag{17}$$

where V_b is the unreduced earthquake force, WT is the total weight, Vs is the base shear force, R is the earthquake reduction coefficient, and Cs is the ratio of base shear force to building weight. Base shear force was calculated as 16970 kN. The ratio of base shear force to building weight was calculated as 10.84%.

The thickness of the steel plate to be placed between the elastomer layers was 2 mm according to the standards. The thickness of one of the layers in the isolator was calculated by Eq. (18), and the shape factor of the isolator was calculated by Eq. (19).

$$\frac{D}{80} \leq t_0 \leq \frac{D}{40} \tag{18}$$

$$S = \frac{\text{Disc Area}}{\text{Cross section area}} = \frac{\frac{\pi \times D^2}{4}}{\pi \times D \times t_0} = \frac{D}{4 \times t_0} \tag{19}$$

where t_0 is the thickness of the rubber between the steel plates and S is the shape factor of the isolator. The thickness of the elastomer layer of the isolator was calculated as 15 mm.

The total elastomer thickness was calculated as 300 mm, one-layer elastomer thickness was calculated as 15 mm, and 20 elastomer layers of elastomer were used. There were 19 steel plates with a thickness of 2 mm. There were 25 mm steel plates on the top and bottom of the isolators. The total isolator height was calculated as 388 mm. A cross-section of isolators with 450 mm diameter is given in Fig. 4. The compression module, E_C, was calculated by Eq. (20), and vertical stiffness, K_V, was calculated by Eq. (21). The stiffness of the steel plate, K, was considered to be 2000 MPa.

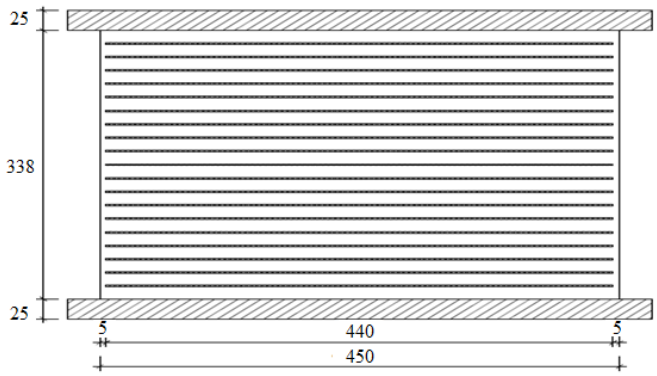

Figure 4. Detail of a selected isolator

$$E_C = \frac{6 \times G \times S^2 \times K}{6 \times G \times S^2 + K} \tag{20}$$

$$K_V = \frac{E_C \times A}{t_r} \tag{21}$$

The total vertical stiffness of all isolators was calculated by Eq. (22).

$$\sum K_V = N \times K_V \tag{22}$$

Total vertical stiffness was calculated as $\mathbf{53 \times 10^6\ kN/m}$. The design displacement of the building, Δt, in the vertical was calculated by Eq. (23), and the vertical vibration period, TV, was calculated by Eq. (24).

$$\Delta t = \frac{W_t}{K_V} \tag{23}$$

$$T_V = \frac{T_{DV}}{\sqrt{6S}} \tag{24}$$

The horizontal displacement was calculated as $\mathbf{24 \times 10^{-4}\ m}$, and the vertical vibration period was calculated as 0.33 s. Eqs. (25-26) were used to calculate the common area of isolators.

$$A' = A\left(1 - \frac{2}{\pi}(\theta + \sin\theta\cos\theta)\right) \tag{25}$$

$$\mathrm{Sin}\theta = \frac{D_D}{D} \tag{26}$$

where D_D is shear displacement and $\mathbf{A'}$ represents the common area when the isolator moves.

The moment of inertia of the rubber bearing section was calculated by Eq. (27), and the control of stability loss was calculated by Eq. (28).

$$I = \frac{\pi \times \left(\frac{D}{2}\right)^4}{4} \tag{27}$$

$$P_{critic} = \frac{\pi}{4}\sqrt{\frac{E_C \times I \times G \times A_S}{3}} \tag{28}$$

where P_{critic} is the load supported by the isolator. Since the values obtained from this calculation were higher than the load supported by the isolator, there was no collapse risk. Post-yield stiffness was calculated by Eq. (29), and elastic stiffness was calculated by Eq. (30).

$$K_2 = \frac{A \times G}{t_r} \tag{29}$$

$$K_1 = 6 \times K_2 \tag{30}$$

where K_2 is plastic stiffness, and K_1 is elastic stiffness. The shear force of the isolator was calculated by Eq. (31).

$$Q = C_S \times W \tag{31}$$

Yielding displacement was calculated by Eq. (32).

$$D_Y = \frac{Q}{K_1 - K_2} \tag{32}$$

where D_y is yielding displacement.
Effective stiffness corresponding to the maximum displacement, K_{eff}, was calculated by Eq. (33).

$$K_{eff} = K_1 + \frac{Q}{D} \tag{33}$$

Yielding strength, F_Y, was calculated by Eq. (34).

$$F_Y = K_1 \times D_Y \tag{34}$$

Mechanical properties of all HDRBs are given in Table 3.

Table 3. Mechanical properties of the HDRB

Column	S1	S2	S3	S4	S5	S6	S7	S8	S9	S10
k_D (kN/m)	256	359	564	718	923	1102	1231	1333	1590	1897
An Isolator Diameter (cm)	45	45	50	55	60	65	70	75	80	90
K_H (kN/m)	530	530	654	792	942	1106	1282	1472	1675	2120
S	7.5	7.5	8.33	9.16	10	10.83	11.66	12.5	13.33	15
$E_C 10^2$ (kN/m^2)	2888	2888	3448	4027	4615	5208	5799	6383	6957	8060
$K_V 10^2$ (kN/m)	1501	1501	2213	3127	4265	5648	7294	9216	1143	1676
Sinθ	0.825	0.825	0.742	0.674	0.618	0.57	0.53	0.494	0.463	0.412
θ	55.63	55.63	47.98	42.48	38.25	34.85	32.05	29.69	27.67	24.38
Radian	0.97	0.97	0.84	0.74	0.666	0.61	0.558	0.516	0.481	0.424
A'	0.013	0.013	0.029	0.049	0.074	0.104	0.137	0.174	0.216	0.311
I (cm^4)	0.0018	0.001	0.002	0.004	0.005	0.008	0.011	0.014	0.019	0.03
P_{critic} (kN)	1717	1717	2590	3747	5232	7094	9381	12141	15422	23735
K_2 (kN/m)	520	520	642	777	924	1085	1258	1444	1643	2079
K_1 (kN/m)	3120	3120	3852	4662	5545	6510	7548	8664	9858	12474
Q (kN)	53	74	117	149	191	229	255	276	330	393
D_y (m)	0.02	0.028	0.036	0.038	0.041	0.042	0.04	0.038	0.04	0.037
K_{eff} (kN/m)	656.9	711.8	943.4	1160.4	1417.7	1674.1	1916.0	2146.9	2493.0	3093.9
F_Y (kN)	63.8	89.31	140.35	179.63	229.66	274.32	306.22	331.74	395.53	472.09

III. RESULTS

The first six periods of the fixed and seismic isolated building obtained from analysis results are given in Table 4. Mode shapes of fixed buildings and seismic isolated buildings with LEC and TEC are shown in Figs. 5-6, respectively. Since the structure was antisymmetric, its first mode was under the torsional effect [25]. The mass participation ratio for each direction is given in Table 5.

Predominant periods of the seismically isolated buildings with LEC and TEC were 2.389 s. and 2.279 s., respectively. The isolator periods for the LEC and TEC buildings were 2.455 s. and 2.334 s., respectively. Analysis results showed that the predominant periods of the seismically isolated building with LEC and TEC were two and a half times longer than the fixed building. The period of the seismically isolated building with TEC was shorter than the building seismically isolated with LEC. This difference is likely because the additional masses of the columns were included in the superstructure when the isolators were located at the bottom.

For the first mode of the fixed building, the mass participation ratio in the X direction was not large compared to the isolated building. The most important reason for this was the torsional effect in the building due to the fact that the stiffness center and the center of mass were not close [26]. The seismic isolation system increased the mass participation ratio in the first mode of the building to approximately 98% and 76% in the X and Y directions. Thus, the torsional effect in the building was reduced with the isolation system [27].

Columns located on the 11-D axis of the building were selected by considering the most favorable load combination to compare the internal column forces of the fixed, seismically isolated buildings with LEC and TEC.

The shear forces and maximum bending moments for the selected columns are shown in Tables 6-7, respectively. V_2 and V_3 represent the horizontal and vertical shear forces of the column section.

Table 4. Periods of fixed and isolated buildings

Mode Number	Fixed (s)	LEC (s)	TEC (s)
Isolator Mode	N/A	2.455	2.334
1. Mode	0.930	2.389	2.279
2. Mode	0.807	2.254	2.156
3. Mode	0.580	0.494	0.488
4. Mode	0.337	0.484	0.477
5. Mode	0.325	0.425	0.421

Table 5. Mass participation ratios of buildings

	X direction			Y direction		
	Fixed Building	Isolated Buildings		Fixed Building	Isolated Buildings	
		LEC	TEC		LEC	TEC
Isolator mode		0.5%	0.4%		75.9%	75.5%
Mode 1	0.5%	99.5%	98.3%	52.7%	76.5%	76.1%
Mode 2	70.3%	99.5%	98.3%	53.4%	99.6%	98.3%
Mode 3	70.5%	99.9%	98.6%	72.3%	99.6%	98.3%
Mode 4	70.6%	99.9%	98.6%	83.2%	99.6%	98.3%
Mode 5	86.2%	99.9%	98.6%	83.2%	99.9%	98.6%

Table 6. Shear forces of the selected columns

FIXED		ISOLATED			
		LEC		TEC	
V_2	V_3	V_2	V_3	V_2	V_3
kN	kN	kN	kN	kN	kN
170	547	107	376	61	314
-8	-548	77	-375	-89	-314
181	547	96	270	60	270
-23	-547	29	-269	-71	-269
142	480	91	238	41	225
29	-481	56	-237	-50	-225
197	422	103	181	52	183
-32	-420	41	-179	-62	-182
164	309	88	126	39	127
-11	-309	47	-125	-42	-126
166	181	120	78	18	76
92	-180	110	-76	-26	-75

FIXED	
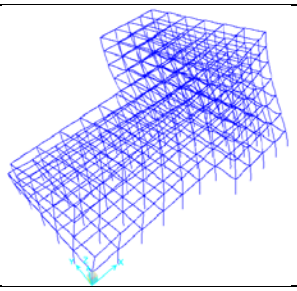	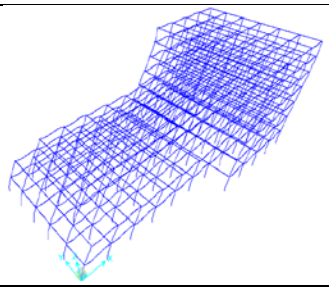
(a) Mod1=0,930 s (Torsional mode)	(b) Mod2=0,807 s (Transverse mode)
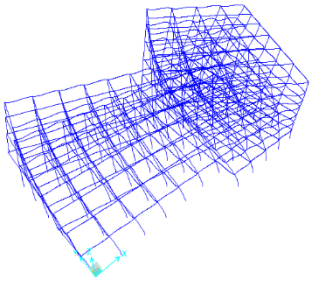	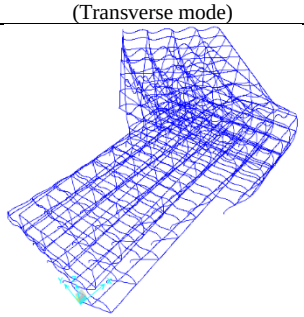
(c) Mod3=0,580 s (Torsional mode)	(d) Mod4=0,337 s (Torsional mode)
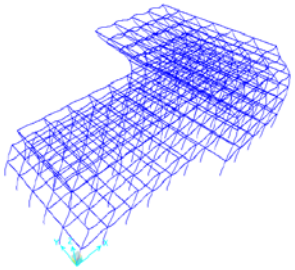	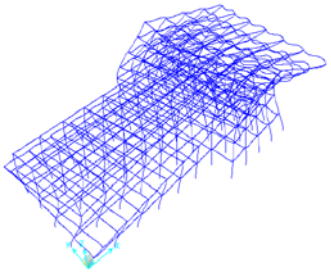
(e) Mod5=0,325 s (Transverse mode)	(f) Mod6=0,299 s (Torsional mode)

Figure 5. Fixed Building Mode Shapes

LEC		TEC	
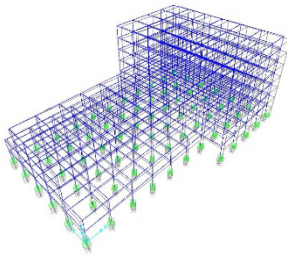	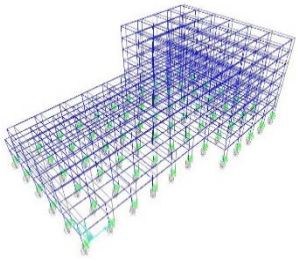	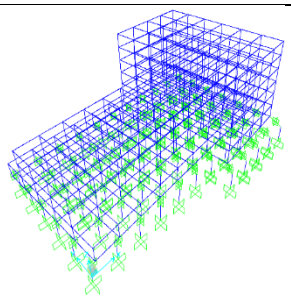	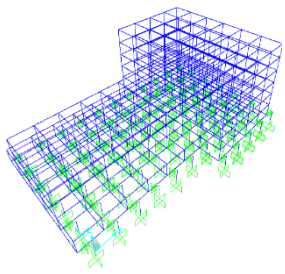
(a) Isolator mode=2,455s (Torsional mode)	(b) Mod1=2,389 s (Transverse mode)	(a) Isolator Mode=2,334 s (Torsional mode)	(b) Mod1=2,279 s (Transverse mode)
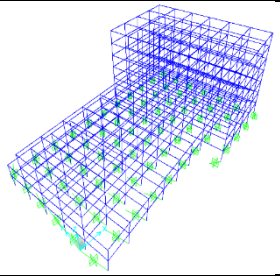	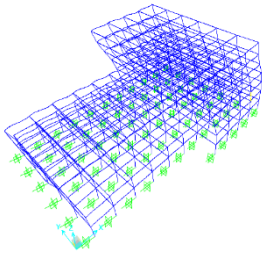	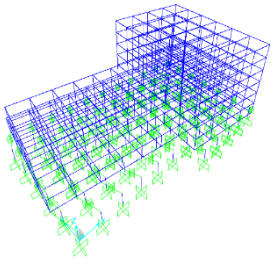	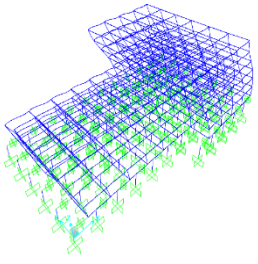

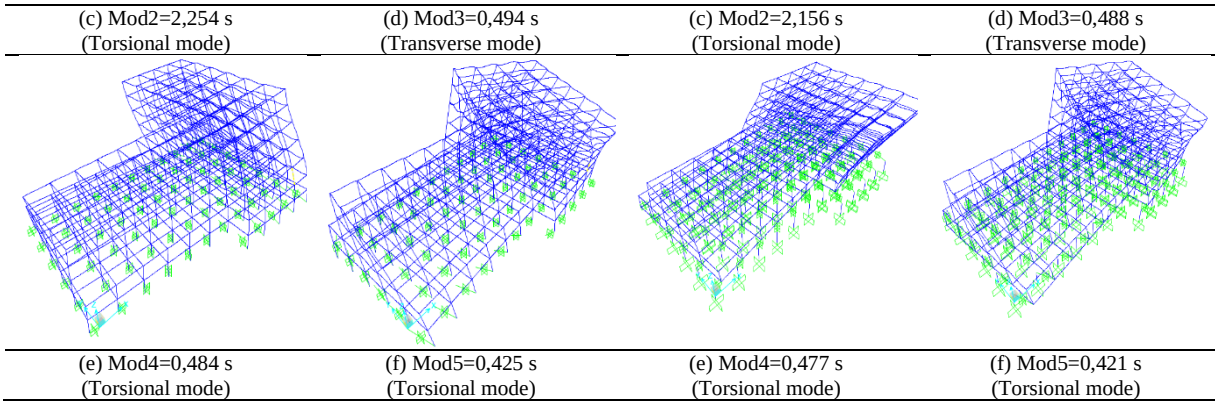

Figure 6. Mode shapes of buildings seismically isolated with LEC and TEC

Table 7. Maximum bending moments of the selected columns

FIXED		ISOLATED			
		LEC		TEC	
M2 (kNm)	M3 (kNm)	M2 (kNm)	M3 (kNm)	M2 (kNm)	M3 (kNm)
2390	-1654	1068	-1009	1228	-1163
2384	-1794	1068	-1025	1228	-1182
1677	-741	899	-508	773	-338
1158	-922	653	-480	595	-393
1505	-949	655	-439	596	-404
1420	-856	561	-360	556	-334
1427	-816	559	-314	406	-311
1305	-992	448	-368	455	-376
1308	-1075	419	-378	432	-387
1060	-1073	334	-338	339	-346
799	-1045	275	-412	285	-408
718	-860	245	-413	247	-408

The seismic reduction coefficient of seismic isolation buildings was selected as 2 according to UBC-97. The seismic reduction coefficient of fixed buildings with 0.93 s was selected as 2 [28]. Choosing the same value for the seismic reduction coefficient gave more accurate results for comparison. However, when the more significant value was selected, the earthquake effect was much less. As a result of the analysis, the shear force on the isolated building with TEC decreased by 40% compared to the fixed building. The shear forces for the building isolated with TEC were approximately 21% less than the building isolated with LEC. The maximum bending moment of the building isolated with TEC decreased by 56% compared to the fixed building. The bending moment of the buildings isolated with TEC and LEC were almost equal to each other.

The base shear forces of the design earthquake in the X and Y directions for the fixed building and buildings isolated with TEC and LEC are given in Table 8.

As a result of the analysis, the base shear forces on the isolated building decreased by approximately 56% and 57% in the X and Y direction, respectively. The base shear force of the building isolated with LEC was approximately 2% and 3.4% less than for the building with TEC in X and Y directions, respectively.

The story drifts in the X and Y directions of the fixed building, and buildings isolated with LEC and TEC are shown in Figs. 7-8 from SAP2000 software.

The relative floor displacement of the buildings isolated with TEC and LEC was approximately 50% less than the fixed building. The total floor displacements of the building isolated with TEC were 5% less than the building isolated with LEC. To better understand the effect of the location of the isolators on the building, a comparison was made by calculating the rebar necessary for LEC and TEC buildings. The necessary rebar of columns in the selected 11 axis of the buildings isolated with TEC and LEC are shown in Table 9.

Since the base shear force of buildings with TEC was higher and its period was shorter, the necessary rebar of column of the isolated 1st floor increased by about 5% compared to the building with LEC. However, this difference only occurred on the first floor of the building. Due to the fewer internal forces in isolated columns and close cross-sectional area on the upper floors of the building, minimum rebar was enough.

The necessary rebar of beams in the selected 10 axis of the buildings isolated with TEC and LEC are shown in Table 10. The rebar of beam decreased by approximately 16% throughout the building isolated with TEC. This ratio was around 15% in the overall building. This shows that the design of the building isolated with TEC was more economical.

Table 8. Base shear forces of the three different analyses

Direction	Fixed (kN)	LEC (kN)	TEC (kN)
X	36707	16221	16581
Y	34768	14755	15273

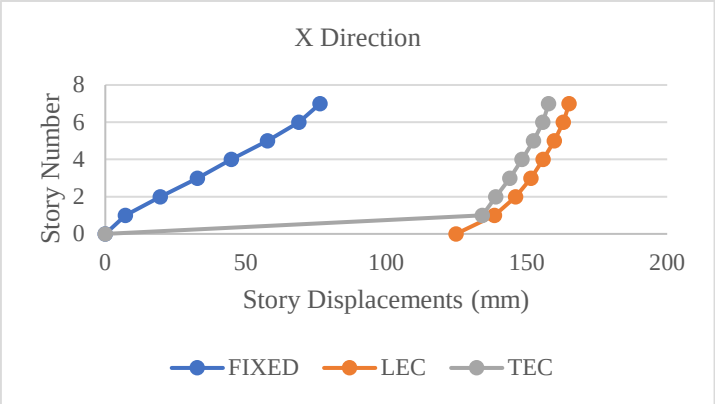

Figure 7. Story drifts in the X direction

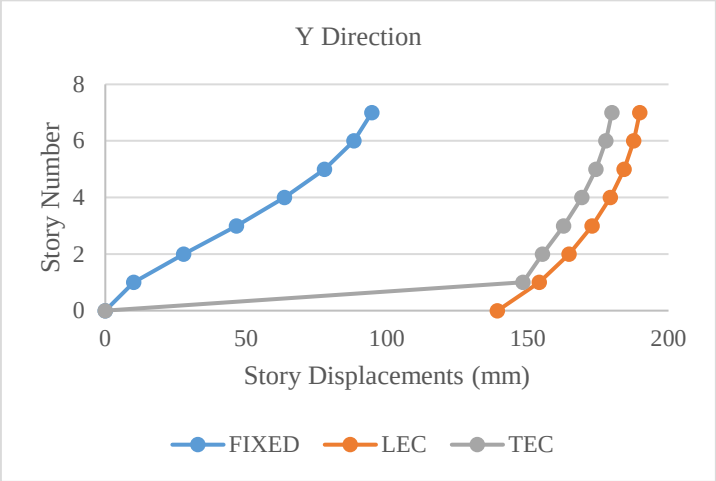

Figure 8. Story drifts in the Y direction

Table 9. Necessary rebar of column in buildings isolated with TEC and LEC

	11 – 11 Axis (mm^2)													
	A		B		C		D		E		F		G	
Floor	TEC	LEC	TEC	LEC	TEC	LEC	TEC	LEC	TEC	LEC	TEC	LEC	TEC	LEC
1	8731	7353	10002	8192	9352	7358	8601	6502	9030	6891	9708	7779	8585	7220
2	6400	6400	6400	6400	6400	6400	6400	6400	6400	6400	6400	6400	6400	6400
3	6400	6400	6400	6400	6400	6400	6400	6400	6400	6400	6400	6400	6400	6400
4	6400	6400	6400	6400	6400	6400	6400	6400	6400	6400	6400	6400	6400	6400
5	6400	6400	6400	6400	6400	6400	6400	6400	6400	6400	6400	6400	6400	6400
6	6400	6400	6400	6400	6400	6400	6400	6400	6400	6400	6400	6400	6400	6400
7	6400	6400	6400	6400	6400	6400	6400	6400	6400	6400	6400	6400	6400	6400

Table 10. Necessary rebar of beam in buildings isolated with TEC and LEC

	10 – 10 Axis (mm^2)					
Floor	A-B axis		B-C axis		C-D axis	
	TEC	LEC	TEC	LEC	TEC	LEC
7	1351	1352	1355	1355	1347	1347
	1177	1177	1082	1082	1085	1085
6	1619	1567	1732	1721	1730	1722
	1136	1137	1083	1083	1082	1082
5	2042	1973	2171	2120	2171	2150
	1148	1149	1083	1082	1084	1083
4	2464	2396	2598	2579	2598	2582
	1165	1150	1224	1215	1224	1217
3	2876	2910	2960	3046	2963	3051
	1357	1384	1381	1444	1382	1446
2	3120	3593	3140	3640	3136	3641
	2637	1951	2485	1945	2468	1945
1	2637	5413	2485	5340	2468	5321
	1241	3553	1174	3405	1166	3409

IV. CONCLUSIONS

In this study, a 7-story reinforced concrete building was selected. HDRB was used as the isolation system. The dynamic behaviour of the building isolated at the top end of the columns was compared to the building isolated at the lower end of the columns at foundation level. In addition, buildings with seismic isolation were compared with a fixed building. As a result of the analysis, the following results were obtained.

- The period of the lower end of columns building was approximately 5% longer than for the top end of the columns building.
- Total floor displacements of the building isolated at the top end of the columns were approximately 5% less than the total displacement of the building isolated at the lower end of the columns.
- The shear forces for columns in the building isolated at the top end of the columns were approximately 21% less than the building isolated at the lower end of the columns.
- Although rebar of column of the building isolated at the top end of the columns were higher by approximately 5% than for the building isolated at the lower end of the columns on the 1st floor, rebar of beam in the whole building isolated at the top end of the columns were less than the building isolated at the lower end of the columns, considering the whole building.
- The base shear force of the building seismically isolated at the top end of the columns was approximately 2.7% more than the building isolated at the lower end of the columns. This result showed that the different locations of the high damping rubber bearing did not lead to a significant difference in the base shear forces.

- The necessary rebar of the beam in the building isolated at the top end of the columns was lower by 15% than for the building isolated at the lower end of the columns.
- Placing the isolator on top of the column may reduce the shear wall required for seismic space and excavation costs in new buildings. However, isolators placed at the lower end of the column may cause various architectural and usage difficulties in the building.
- The mass participation ratio increased in the first mode of the seismic isolation system for an asymmetrical building. This situation revealed that the seismic isolation system dramatically reduced the torsional effect in this building.

Based on all these results, it is more economical to place the seismic isolator at the top of the column in such a building considering the total rebar areas. In addition, from an architectural point of view, it is more appropriate to place seismic isolators at the top end of the column.

REFERENCES

1. Ryan KL and Earl CL (2010) Analysis and Design of Inter-Story Isolation Systems with Nonlinear Devices. Journal of Earthquake Engineering 14(7):1044–1062. https://doi.org/10.1080/13632461003668020
2. Huang XY, Zhou FL, Wang L, Heisha LHW and Luo XH (2011) Experimental Investigation on Mid-Story Isolated Structures. Advanced Materials Research 163–167: 4014–4021. https://doi.org/10.4028/www.scientific.net/AMR.163-167.4014
3. Shahzad MM, Zhang XA, Wang X, Abdulhadi M, Wang T and Xiao Y (2022) Response control analysis of a new mega-subcontrolled structural system (MSCSS) under seismic excitation. The Structural Design of Tall and Special Buildings, 31(10), e1935. https://doi.org/10.1002/tal.1935
4. Shu T, Li H, Wang T, Liu D, Yao S and Lei M (2023) Study on the seismic response of new staggered story isolated structure under different parameters. Frontiers in Earth Science, 11, 1115235. https://doi.org/10.3389/feart.2023.1115235
5. Di Egidio A, Pagliaro S, and Contento A (2023) Seismic Performance of Frame Structure with Hysteretic Intermediate Discontinuity. Applied Sciences, 13(9), 5373. https://doi.org/10.3390/app13095373.
6. Skandalos K, Afshari H, Hare W, and Tesfamariam S (2020) Multi-objective optimization of inter-story isolated buildings using metaheuristic and derivative-free algorithms. Soil Dynamics and Earthquake Engineering, 132, 106058. https://doi.org/10.1016/j.soildyn.2020.106058.
7. Charmpis DC, Komodromos P and Phocas MC (2012) Optimized earthquake response of multi-storey buildings with seismic isolation at various elevations. Earthquake Engineering & Structural Dynamics 41(15): 2289–2310. https://doi.org/10.1002/eqe.2187
8. Zhou FL, Zhang Y and Tan P (2009) Theoretical study on story isolation system. China Civil Engineering Journal 42(8): 1–8. https://doi.org/10.1016/j.engstruct.2020.111296
9. Wang SJ, Chang KC, Hwang JS and Lee BH (2011) Simplified analysis of mid-story seismically isolated buildings. Earthquake engineering & structural dynamics 40(2): 119-133. https://doi.org/10.1002/eqe.1004
10. Wang SJ, Chang KC, Hwang JS, Hsiao JY, Lee BH and Hung YC (2012) Dynamic behavior of a building structure tested with base and mid-story isolation systems. Engineering Structures 42: 420–433. https://doi.org/10.1016/j.engstruct.2012.04.035
11. Kim HS and Kang JW (2019) Optimal design of smart mid-story isolated control system for a high-rise building. International Journal of Steel Structures. https://doi.org/10.1007/s13296-019-00258-8
12. Faiella D and Mele E (2020) Insights into inter-story isolation design through the analysis of two case studies. Engineering Structures 215. https://doi.org/10.1016/j.engstruct.2020.110660
13. Becker Tracy C and Ezazi Ashkan (2015) Enhanced performance through a dual isolation seismic protection system. The Structural Design of Tall and Special Buildings 25(1): 72-89. https://doi.org/10.1002/tal.1229
14. Xiao S, Li C, Liu D, Sun W and Lei M (2023) Research on Irregular Plane Mid story Isolation Structures in Castor Earthquake prone Areas Considering SSI Effect. Frontiers in Earth Science 11. https://doi.org/10.3389/feart.2023.1207110
15. Zhou Q, Singh MK and Huang X (2016) Model reduction and optimal parameters of mid-story isolation systems. Engineering Structures 124: 36-48. https://doi.org/10.1016/j.engstruct.2016.06.011
16. Kim HS and Kim U (2023) Development of a Control Algorithm for a Semi-Active Mid-Story Isolation System Using Reinforcement Learning. Applied Sciences 13(4) 2053. https://doi.org/10.3390/app13042053

17. Zhang R, Phillips BM, Taniguchi S, Ikenaga M and Ikago K (2017) Shake table real-time hybrid simulation techniques for the performance evaluation of buildings with inter-story isolation. Structural Control and Health Monitoring 24(10). https://doi.org/10.1002/stc.1971
18. Wu Y, Lu J and Qi A (2019) Shaking table test and numerical analysis of mid-story isolation eccentric structure with tower–podium. Advances in Mechanical Engineering 11(1). https://doi.org/10.1177/1687814018819562
19. Uniform Building Code 1997 American Structural Engineering Design Provisions.
20. Saifullah MK and Alhan C (2017) Necessity and adequacy of near-source factors for seismically isolated buildings. Earthquakes and Structures 12(1): 91-108. https://doi.org/10.12989/eas.2017.12.1.091
21. General Directorate for Foundations 2018 Turkey Building Earthquake Code (TBEC2018).
22. Soyluk A and Tuna ME (2011) Effect of seismic base isolation usage on the architectural design of irregular buildings. Journal of the Faculty of Engineering and Architecture of Gazi University 26(3):635-642
23. Farmanbordar B, Adnan AB, Tahir MM and Faridmehr I (2017) Seismic assessment of base-isolated nuclear power plants. Advances in computational design 2(3): 211-223. https://doi.org/10.12989/acd.2017.2.3.211
24. Design loads for buildings 1997 Turkish Standard Code 498
25. Taha AE, Elias S, Matsagar V and Jain KJ (2019) Seismic response control of asymmetric buildings using tuned mass dampers. Structural Design of Tall and Special Building. 28(18). https://doi.org/10.1002/tal.1673
26. Orak MS and Celep Z (2017) Seismic Performance of Gedikbulak School Building Revisited. Teknik Dergi. 28(2): 7889–7889. https://doi.org/10.18400/tekderg.304103
27. Kilar V and Koren D (2009) Seismic behaviour of asymmetric base isolated structures with various distributions of isolators. Engineering Structures 31(4): 910–921. https://doi.org/10.1016/j.engstruct.2008.12.006
28. Tsiavos A, Schlatter D, Markic T and Stojadinovic B (2017) Experimental and analytical investigation of the inelastic behavior of structures isolated using friction pendulum bearings. Procedia Engineering 199: 465–470. https://doi.org/10.1016/j.proeng.2017.09.047